The use of portable XRF as a forensic geoscience non-destructive trace evidence tool for environmental and criminal investigations

J.K. Pringle[a,*], A.J. Jeffery[a], A. Ruffell[b], I.G. Stimpson[a], D. Pirrie[c], E. Bergslien[d], C. Madden[a], I. Oliver[a], K.D. Wisniewski[f], J.P. Cassella[e,g], N. Lamont[e], S. Gormley[b], J. Partridge[e]

[a] School of Geography, Geology & Environment, Keele University, Keele, Staffordshire ST5 5BG, UK
[b] School of the Natural Built Environment, Queens University, Belfast, Northern Ireland BT7 1NN, UK
[c] School of Applied Science, University of South Wales, Pontypridd, Rhondda Cynon Taff CF37 4AT, UK
[d] Earth Sciences and Science Education, 165 Science Building, 1300 Elmwood Ave., Buffalo, NY 14222, USA
[e] Department of Criminal Justice and Forensics, School of Law, Policing & Forensics, Science Centre, Staffordshire University, Leek Road, Stoke on-Trent, Staffordshire ST4 2DF, UK
[f] School of Chemical & Physical Sciences, Keele University, Keele, Staffordshire ST5 5BG, UK
[g] Department of Life Sciences, School of Science, Institute of Technology Sligo, Ash Lane, Ballinode, Sligo F91 YW50, Ireland

ARTICLE INFO

ABSTRACT

Hand-held, portable X-Ray fluorescence instruments (pXRF) provide a means of rapid, in-situ chemical characterisation that has considerable application as a rapid trace evidence characterisation tool in forensic geoscience. This study presents both a control test study which demonstrates optimisation of the data collection process, alongside a range of individual forensic case studies, including heavy metal contamination, conflict archaeology, forensic soil characterisation, and verification of human remains, which together validate the technique and provide some comparison between field-based and laboratory-based pXRF applications. Results highlight the time-efficiency and cost-effectiveness of in-situ, field-based pXRF analyses for material characterisation when compared with other trace evidence methods. Analytical precision of various analytes during in-situ analysis was sufficient to demonstrate considerable application of field-based pXRF as a tool for rapid identification of specific areas of interest to be further investigated. Laboratory-based pXRF analyses yielded greater accuracy which could provide an efficient compromise between field-based pXRF and traditional laboratory-based analytical techniques (e.g. WD-XRF, ICP-MS). Further studies should collect more advanced datasets in more diverse locations to further validate the techniques capability to rapidly conduct geochemical surveys in a range of environments.

1. Introduction

Forensic geoscience trace evidence is widely used to assist in both criminal and environmental investigations and includes the analysis of naturally occurring geological/soil material and man-made products constructed from geological raw materials (e.g. [1,2]). This trace evidence may be transferred to items such as vehicles, clothing or footwear during a criminal act [3], or the illegal disposal of waste materials may lead to their increased abundance in soils or sediments [4]. The most commonly analysed types of geoforensic trace evidence are soils [5], sediments, dusts or rock fragments [5,6] or construction materials (e.g. concrete) [1] with common analytical laboratory analysis undertaken either characterising the materials chemistry through, for example, ICP [7,8], INAA [9], LIBS [7,10] and XRF [11] or its mineralogy using methods such as XRD [12,13] manual scanning electron microscopy [14] or automated electron microscopy (e.g. [1]). In these cases, crime scene assessment and sampling is carried out with the samples returned for subsequent laboratory analysis [2]. However, in certain civil or criminal investigations where rapid forensic object identification or site characterisation is required, often within a restricted time period, it may be necessary for relatively rapid field surveys to be undertaken alongside sampling for laboratory analysis. Rapid field survey techniques include measurements of biological samples (see [15]), and physical properties including geochemistry, for example

* Corresponding author.
E-mail addresses: j.k.pringle@keele.ac.uk (J.K. Pringle),
a.j.jeffery@keele.ac.uk (A.J. Jeffery), a.ruffell@qub.ac.uk (A. Ruffell),
i.g.stimpson@keele.ac.uk (I.G. Stimpson), duncan.pirrie@southwales.ac.uk (D. Pirrie),
bergslet@buffalostate.edu (E. Bergslien), cassella.john@itsligo.ie (J.P. Cassella),
N.A.Lamont@staffs.ac.uk (N. Lamont), s.gormley@qub.ac.uk (S. Gormley),
j.d.partridge@staffs.ac.uk (J. Partridge).

colourimetric soil tests to detect TNT [16], mineralogy using for example Raman spectroscopy [17] and near-surface geophysics which includes magnetic susceptibility soil characterisation studies (see [18,19]).

X-ray fluorescence spectrometry (XRF) is a fundamental analytical technique for the chemical characterisation of geological and environmental materials. The advent of field-portable XRF instrumentation (often abbreviated as pXRF, fpXRF, or hXRF) provides a means of rapid, in-situ chemical characterisation, which has been applied to a variety of subject areas, including: mineral exploration (e.g. [20]), geology (e.g. [21]), environmental science (e.g. [22]), archaeology (e.g. [23, 24]), and the arts (e.g. [25]). Although traditional, laboratory-based, wavelength dispersive XRF will undoubtedly remain the analytical method of choice for studies in which data must be of the highest possible quality, such analyses inevitably involve greater costs, lengthier preparation procedures, and longer analysis times. The greatest strengths of pXRF are the speed with which large volumes of data can be collected and the reduced amount of sample preparation required, which may range from none (in-situ, non-destructive analysis) to extensive (sample collection, homogenisation, and pelleting), at the user's discretion.

Portable XRF (pXRF) field surveys have been shown to be effective for rapid evaluation of heavy metal soil contamination [22,26,27,28], living biogeochemical mapping over mine tailings [29], archaeological object studies [30,31], marine microplastics [32] and even lead levels in living human bones [33] and species profiling [34]. The applications of portable XRF and the requirements in terms of analytical methodology have been considered extensively in the archaeological science literature. Whilst it is widely recognised that some elements (e.g. Na, P, V etc) cannot be accurately quantified using portable XRF at the concentrations at which they are usually present [35] the ability to carry out in-situ analysis for other elements, means that the methodology has considerable application as a field-based analysis tool [36].

Soil moisture content is a major variable, both within an individual study site as well as for comparison between different sites, especially for physical measurements e.g. electrical resistivity surveys (see [37]). This holds true for pXRF analysis, with the additional complication that water attenuation of X-rays is a function of their energy that are used to characterize the elements of interest. Low-energy X-rays are more strongly attenuated than high-energy ones, thus for pXRF analysis, elements with lower atomic masses are more strongly impacted. Studies have shown that for every 1% increase in soil moisture, there is a 1.15 – 1.75% decrease in reported elemental concentration for manganese through to arsenic, while elements lighter than Mn are even more greatly attenuated [38,39]. This means that sample moisture content must be taken into account, as light element values determined in situ will likely not be directly comparable to results of a traditional laboratory analysis [40]. As this is a known, it can be adjusted for when a rapid field assessment is required.

This paper aims to (1) validate the potential application of portable XRF instruments for surface surveys as a forensic trace evidence technique through six illustrative case studies with varying objectives, study sites and outcomes; (2) through a case study comparing portable XRF with laboratory-based XRF analysis and (3) suggest best practice for pXRF surveys in a forensic context.

2. Case studies

This section will detail seven different studies, four field-based and three laboratory-sample based measurements. Different pXRF instruments were used in these case studies and their relative specifics, sample measurement time and detection limits are given in Table 1 below.

2.1. pXRF measurement duration test

Prior to field analysis and sample collection, the effect of analysis time on analytical precision and accuracy was quantified, the aim of which was to determine a compromise between time required for analysis and data resolution. The actual resolution required will inevitably be specific to the analytical requirements of each individual application, and the user(s) must balance individual analysis time with the overall number of analyses required. For this study, this relationship was evaluated using a single surface soil sample collected from St. John's church graveyard in Keele, Staffordshire, U.K., which was analysed in the same location using 5 different total analytical times (1–5 min; Fig. 1), using a ThermoScientific™ NITON XL3t 900 Analyzer that costs ~£ 30,000 and weighs 1.9 Kg. This sample was selected as a reasonable representative of the samples being analysed in this study. The instrument employs four sub-filters (Main, Low, High, Light), each targeting a specific range of elements. Each of these filters was allotted an equal proportion of the overall analytical time (i.e. a 4 min analysis with 1 min allotted to each filter).

Prior to analysis, the sample was oven-dried for 24 h at 105 °C before being hand-ground using a pestle and mortar to pass through a 63 μm sieve. It was then mixed with 1.5 mL of poly-vinylpyrrolidone-methylcellulose binding agent, mechanically pressed under 10 Tn pressure into a homogenous flat-cylinder pellet, before being oven dried for a further 24 h at 105 °C to remove any moisture influence on signal strength [41].

The relationship between analysis duration and two-sigma error margins (determined by the instrument's internal software via counting statistics) is shown for selected elements in Table 2 and Fig. 1. For the selected elements, the greatest improvement in error lies between 60 and 120 s. Errors for Pb, Zn, Mn, and Sr were lower than 20% relative using a 120 s analysis time, but, using a 300 s analysis time could be reduced to <10% relative for Sr, Mn, and Pb, and < 15% relative for Zn. As such, due to the time constraints of field working, a 120 s analysis time was selected for field-based analyses. For laboratory-based analyses, a 300 s analysis time was selected to provide the lowest possible error.

Analytical precision and accuracy were evaluated using a randomly selected, unprepared soil sample from St. John's church, and a range of international standard reference materials (NIST 2780, BHVO-1, AC-E, AGV-1). On the basis of repeat measurements, laboratory-based analyses typically yielded precision (expressed as relative 2 sigma standard deviation) within 7% for Zn, 6% for Mn, 4% for Pb, 16% for Cr, and 1% for Sr. In contrast, hand-held analyses indicated precision within 11% for Zn, 7% for Mn, 4% for both Pb and Sr and 25% for Cr. Typical accuracy (expressed as average percentage deviation from known values) for laboratory analyses was within 8% for Zn, 3% for Mn, 3% for Pb and 10% for Sr. Accuracy during hand-held analysis was found to be variably affected by the method for the elements given above, with deviation from known values ranging from 23% to 93%. Accuracy for Cr was unacceptable for concentrations lower than ~100 ppm in both hand-held and laboratory analyses. This demonstrates that actual quantitation in the field using the factory standard calibration should be undertaken with the utmost caution, at least at the relatively low concentrations observed in this study. Ideally, a user-specific calibration should be implemented if field quantitation is required, although this may still be subject to the same problems with proximity to detection limits. Nevertheless, analytical precision achievable during hand-held analysis in the field clearly demonstrates the validity of relative comparison of concentrations during fieldwork, facilitating rapid reconnaissance mapping of an area to identify geochemical highs and lows.

This initial pXRF time duration test case study showed more accurate pXRF measurements could be obtained as sample analysis

Table 1
pXRF instrument specifications, measurement time and detection limits for the 7 case studies presented in this paper.

Case study	Instrument	Detector	Tube type	Tube voltage	Filters	Sample measurement time (s)	Detection limit (ppm)
2.1 Laboratory duration test	Thermo-Scientific™ NITON XL3t 900 Analyzer	Geometrically optimised large area drift detector	Ag anode 50 kV and 200 µA - single tube	6–50 kV	Poly-propylene sub-filters (Main, Low, High, Light)	60	Sr = 4, Pb = 18, Zn = 19, Mn = 148
						120	Sr = 4, Pb = 12, Zn = 14, Mn = 102
						180	Sr = 3, Pb = 10, Zn = 11, Mn = 85
						240	Sr = 3, Pb = 9, Zn = 9, Mn = 72
						300	Sr = 2, Pb = 8, Zn = 8, Mn = 64
2.2 Industrial contam-ination site	Thermo-Scientific™ NITON XL3t 900 Analyzer	Geometrically optimised large area drift detector	Ag anode 50 kV and 200 µA - single tube	6–50 kV	Poly-propylene sub-filters (Main, Low, High, Light)	120	As = 48, Pb = 69, Zn = 113, Cu = 40, Fe = 907, Mn = 157, P = 136, S = 271
2.3 WW1 Conflict study	Thermo-Scientific™ NITON XL3t 900 Analyzer	Geometrically optimised large area drift detector	Ag anode 50 kV and 200 µA - single tube	6–50 kV	Poly-propylene sub-filters (Main, Low, High, Light)	120	Cd = 17, Cu = 23, Ba = 71, Mn = 111, Sr = 4, Pb = 12, Zn = 17
2.4 Missing persons case	Bruker Instruments Tracer 5	Silicon Drift Detector	Be	50 kV	Five position low to high	120	Fe = 50, Na = 290, Mg = 100, Al = 134
2.5 Medieval lignite bangles study	Bruker S1 Turbo LE	10 mm X-Flash	Rh	45 kV	Five automatic	240	Cr = 60, Cd = 40, Pb = 10–60
2.6 Cremated remains test	Niton XL3t GOLDD+	Si PiN detector (FYI - GOLDD stands for Geometrically optimized large area detector – they are still a type of Si PiN detector)	Ag anode X-ray tube	6–50 kV	Poly-propylene sub-filters (Main, Low, High, Light)	270	Ca = 150, Cu = 15, Fe = 50, K = 150, Mn = 60, P = 400, Pb = 10, S = 300, Sr = 10, Zn = 12
2.7 Graveyard soil study	Thermo-Scientific™ NITON XL3t 900 Analyzer	Geometrically optimised large area drift detector	Ag anode 50 kV and 200 µA - single tube	6–50 kV	Poly-propylene sub-filters (Main, Low, High, Light)	120 (field)	Sr = 4, Pb = 14, Zn = 21, Mn = 100, Cr = 14
						300 (lab)	Sr = 3, Pb = 8, Zn = 14, Mn = 67 Cr = 13

time increases which is straight forward, but importantly it showed that a 120 s duration for surface sampling positions and 180 s duration for laboratory measurements gave optimal repeatability and reliability, without being too onerous for the data acquisition team to collect if longer sampling times were required. Comparisons of field versus laboratory measurements of the graveyard soil sample also showed relative concentrations were similar, proving that rapid field surveys are valid for reconnaissance studies before follow-up more detailed sampling and laboratory sample analysis are

undertaken. Clearly, field-based in-situ analysis could be used as a tool to guide sampling for subsequent laboratory analysis.

2.2. Industrial contamination case study: Phoenix Works, Stoke-on-Trent, Staffs, UK

Stoke-on-Trent, Staffordshire, was the home of the UK pottery industry, producing a variety of high-quality ceramic pottery ware from the early 18th to the end of the 20th Century, due to the local
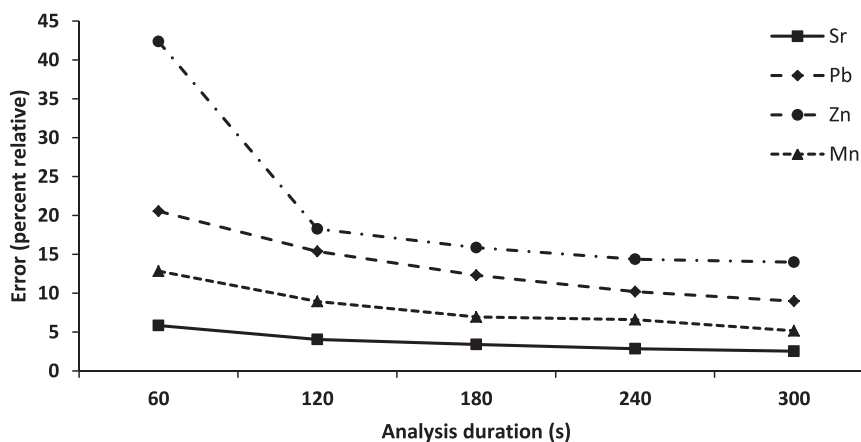
Fig. 1. Relationship between error (% relative) and analysis duration for selected elements in a sample from a Staffordshire church graveyard soil sample (see text).

Table 2
Relationship between analysis time in seconds and 2σ error margins, demonstrated using a randomly selected sample from a Staffordshire church graveyard. All concentrations given in ppm.

Analysis duration (s)	Sr	+/-	Pb	+/-	Zn	+/-	Mn	+/-
60	63	4	34	7	26	11	761	98
120	67	3	33	5	47	9	788	70
180	63	2	33	4	44	7	834	58
240	64	2	34	4	41	6	724	48
300	65	2	35	3	37	5	858	44

availability of clay, salt, lead and coal. Hundreds of companies produced all kinds of pottery, from tablewares and decorative pieces to industrial items. There were up to 4000 different small-scale industrial buildings called bottle kilns (named after their shape – see Fig. 2) that were used to put the pottery ware inside and then heat up and glaze the ceramics, typically over a period of several days, all of which were structurally unique, as they were individually built by their respective company owners. The 1956 Clean Air Act marked the end of their use in the UK. The current Ceramic Heritage Action Zone (HAZ) project is now documenting the surviving 47 pottery kiln buildings which are listed as historically important in the UK. The largest group are found in the Phoenix Works in Longton, Stoke-on-Trent and are the focus of this study.

A ground-based Pheron digital camera scan survey was used to document and record the historically listed Phoenix Works heritage site, but there was also concern about the possible presence of heavy metal contamination within and around the kilns that may be hazardous for the survey teams, especially as the repeated 1000 + °C firing process will have coated the inside of the kilns with a variety of ceramic products, including lead paint, and the coal, wood or other combustibles used for firing them.

A reconnaissance forensic environmental investigation was therefore undertaken, using a pXRF ThermoScientific™ NITON XL3t 900 Analyzer, on 15 sample locations adjacent and within two bottle kiln industrial buildings that were present onsite, with 4 pXRF measurements taken from the bare brick walls and 11 pXRF measurement on the bare brick floors in-situ (see Fig. 2). Each measurement was recorded at 2 min duration and calibrated to the control samples as per the initial 2.1 case study duration suggestions (Table 3).

Heavy metal element concentrations of concern were lead (380–5395 ppm, 2185 ppm average) and arsenic (55–125 ppm,

35 ppm average), with average lead concentrations being at least twice as high on the kiln walls (4330 ppm), when compared to the floor (1400 ppm) location samples (Table 3). After data analysis, it was however, considered safe to undertake the ground-based survey to document the site as element concentrations were not deemed to be high enough to preclude the short time required onsite to conduct the digital survey scans.

This relict industrial contamination case study indicated that rapid in-situ field surveys could give relative concentrations of elements, and confidence that digital surface scans could be completed without harming the data acquisition survey team members for the short time that they were onsite. As such the rapid in-situ analysis becomes part of a site-specific risk assessment, prior to carrying out further analysis or sampling which may expose those carrying out the work to potential contaminants. It would have been useful to undertake a more comprehensive sampling methodology to give more comprehensive site information but it wasn't possible in this case due to time constraints.

2.3. Conflict Archaeology case study: WW1 Hawthorn Crater, Messines Ridge, France, Western Front

Past military conflicts can often leave a site legacy for significant periods after the battles have moved on, with repercussions for the local population, not just for UXO hazards, but also long-lasting soil contamination [42]. One such site investigated is Hawthorn Ridge Crater, found in Beaumont Hamel, France. In WW1 it was a German front-line fortification mined by the Allies, with the mine blown on the first day of the Battle of the Somme on the 1st July 1916, famously filmed by Geoffrey Malins [43]. The remaining surface crater is still present to this day, surrounded by local arable farm land.
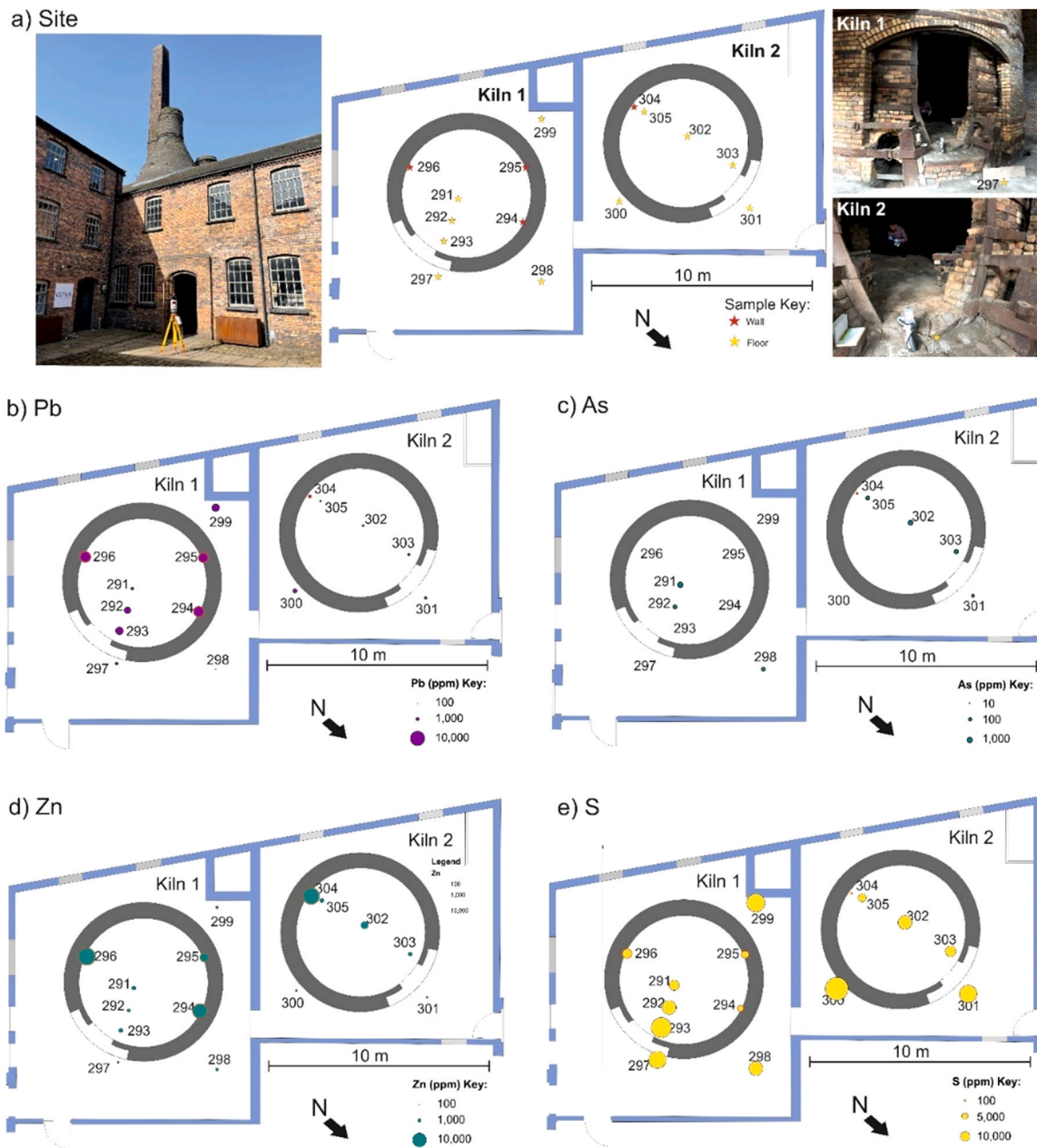
Fig. 2. Phoenix Works pottery bottle kiln industrial building project, Longton, Stoke-on-Trent, Staffordshire, UK. a. site overview, showing (left to right) photograph of works and ground-based scanner in foreground, sitemap showing the 2 kilns, sample locations (see key) and kiln photographs with pXRF ThermoScientific™ NITON XL3t 900 instrument in foreground. b. lead, c. arsenic, d. zinc e. sulphur measured (2 min duration) element concentrations (see keys). Note samples 294, 295, 296 and 304 were acquired on the bottle kiln walls, the others were on the floor.

It was reported that poor plant growth was consistently experienced adjacent to Hawthorn Crater, possibly due to local soil contamination associated with the past conflicts, including heavy metals from spent ordinance, and the mine ammonal and mercury fulminate explosives, hence the focus of this study.

Three surface soil samples (up to 15 cm deep) were taken from an area of visibly poor plant growth, a further five from an area of good plant growth and finally a further five samples taken at 10 m intervals away from the crater edge (Fig. 3). Samples were then prepared for pXRF analysis as per the first case study, i.e. sieved, dried and made into pellets before being analysed by the pXRF Thermo-Scientific™ NITON XL3t 900 instrument for 2 min.

pXRF measurement results show relatively high values of Ba and Sr (Table 4) which are known to affect plant growth [44]. There were surprisingly low concentrations of Cd and Cu, possibly due to the now-arable fields being regularly tilled. Mg, Ba and Sr element concentrations decrease progressively away from the crater (Fig. 4), which suggests that their distributions were related to the crater rather than to the general battlefield.

This conflict archaeology case study evidenced that, despite the opinion that this heavily fought over area in the Western Front had contaminated soil due to the number of spent munitions used and still being found, heavy metals were not in fact very high and the area was thus still suitable for arable crop production. There were

Table 3
pXRF selected element concentrations (ppm) measured over 120 s in situ in two bottle kiln industrial buildings in the Phoenix Works, Longton, Stoke-on-Trent, Staffs, UK (see Fig. 2 for sample locations). See Table 1 for detection limits.

| Reading No	As	Pb	Zn	Cu	Fe	Mn	P	S
291	95	820	1,260	170	46,370	615	5,870	11,650
292	65	2,840	885	376	30,735	1,445	1,400	19,350
293	–	3,500	1,390	168	75,495	1,080	985	36,030
294	–	5,395	11,560	160	35,170	705	1,945	4,715
295	–	5,190	5,460	135	55,530	880	1,745	6,535
296	–	5,955	14,910	184	46,660	805	640	9,610
297	–	750	440	127	73,725	1,160	480	27,615
298	35	640	840	144	43,405	570	1,005	19,970
299	–	3,395	655	110	42,825	740	675	30,550
300	–	1,415	500	139	60,265	460	465	44,665
301	40	670	470	104	31,835	435	695	28,520
302	80	435	3,520	170	82,020	1,080	4,175	18,830
303	65	580	1,250	180	84,410	950	1,175	12,185
304	35	790	14,025	170	47,495	655	970	795
305	60	385	1,395	139	64,475	580	805	7855
average	**30**	**2,185**	**3,900**	**165**	**54,695**	**810**	**1,535**	**18,590**
av. floor	40	1,400	1,145	166	57,780	830	1,610	23,385
av. wall	10	4,330	11,490	162	46,215	760	1,325	5,415
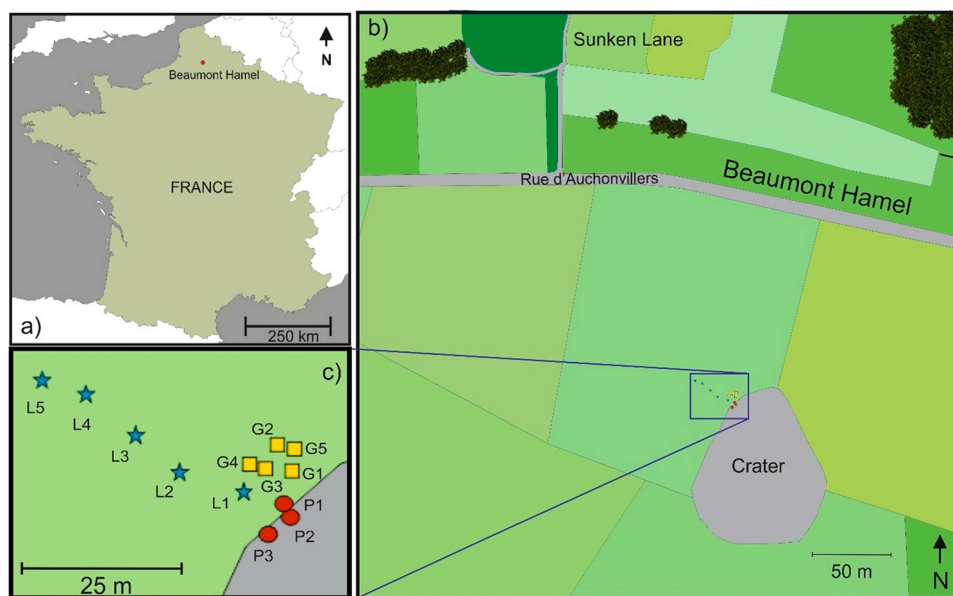
Fig. 3. The Hawthorn Crater study site, Beaumont Hamel, Northern France. a. location map. b. Sitemap showing Beaumont Hamel village to East of Hawthorn Crater, 'sunken lane' Allied forces approach and post-war memorial. c. Sitemap showing pXRF soil sample locations split into poor plant growth (P), good plant growth (G) and along a 10 m transect away from the crater (L).

Table 4
pXRF selected heavy metal element concentration measurement (120 s) averages from the Hawthorn Crater study (see Fig. 3 for locations and text for details). See Table 1 for detection limits.

SAMPLE	XRF Reading (ppm)						
	Cd	Cu	Ba	Mn	Sr	Pb	Zn
Line Average	25	–	80	900	85	40	120
Poor Plant Growth	–	–	130	315	280	15	60
Good Plant Growth	–	–	155	365	200	25	60

interesting decreasing trends away from the crater which was formed due to underground explosives being detonated rather than due to the general battlefield. Other comparable conflict archaeology studies (e.g. [45]) have shown the usefulness of pXRF reconnaissance surveys for follow-up higher resolution surveys or indeed comparison with geophysical survey data [45].

2.4. Suspected murder trace evidence case study: Northern Ireland

This case study is based on an investigation into a suspected murder, in which the victim's body has not been recovered. An individual involved in minor drug-dealing from a town in the north-west of Northern Ireland met his daughter and borrowed some
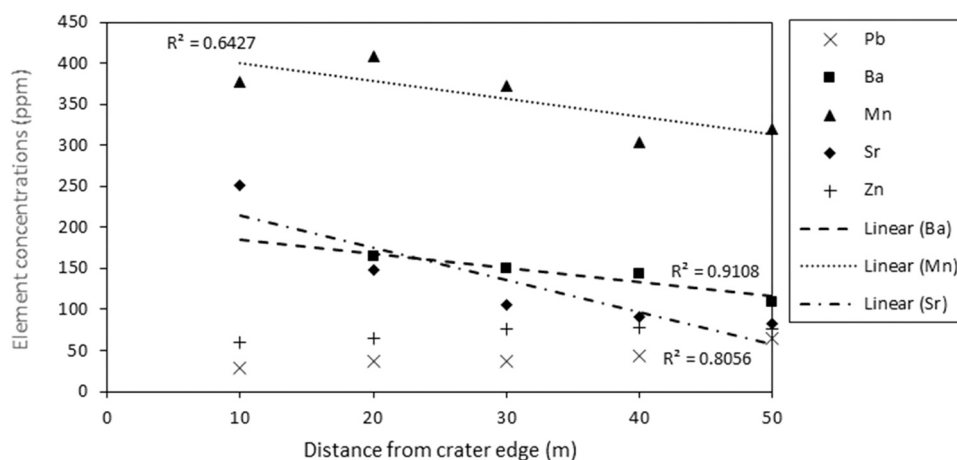
Fig. 4. Graph cross-plot showing selected element (see key) concentration distributions against distance from Hawthorn Crater edge, Beaumont Hamel, Northern France (see text).

money from her, stating that she would be paid back in one week's time, as he had some work imminently. After two weeks had passed, there was no sign of the individual and he was reported as a missing person (the 'Misper' of missing persons enquiries). Around the same time as this missing person report, security officials at Dublin Airport in the Republic of Ireland, noticed a vehicle with a flat tyre that had remained parked, away from other vehicles. On checking the vehicle, they noted that the rear seats seemed to be heavily stained: a number plate check showed this vehicle was registered to the missing person. The vehicle was taken to an Irish Police facility where the stain was confirmed to be blood and the same type as the missing person. A check of CCTV, ANPR and emergency services reports in a transect of likely routes between the MISPER home locale and Dublin Airport only produced one CCTV sighting of the vehicle, on a route between the home address and the airport (Fig. 5). The timing of the CCTV sighting was coincident with the time at which a police vehicle stop of local drug-dealers, in their own vehicles, had also occurred.

The CCTV image of the vehicle was not clear enough to distinguish who was driving the vehicle or how many individuals were inside, but items associated with the Misper, as well as the car park ticket to the airport, showing the date and time of entry, were present within the vehicle. The vehicle had entered the car park some 9 h after it was last sighted on the CCTV image and the corresponding police drug-dealer report. With no other DNA/fingerprint evidence associated with the vehicle, and only one CCTV sighting, the main question was where had the vehicle been in the 9 h between the CCTV sighting and the entry of the vehicle at the car park? The vehicle was therefore brought to Northern Ireland and examined by officers from the forensic laboratory, who noted soil in, and on, various parts of the car.

The vehicle was examined and the presence of soil was confirmed within the engine compartment, on the suspension and wheel-inners, as well as various 0.5–1 cm diameter and some 2 cm wide and 5–15 cm long areas on the window sills and door surrounds (Fig. 5): these were interpreted to be mud-spatter marks, mapped and removed for analysis. The underside soil was measured in situ using pXRF and also removed; in total six samples were collected from the vehicle. Control samples of possible vehicle contact points (puddles, loose verges etc) were also collected around the missing person's home address (eleven samples); his daughter's house (nine samples); similar types of location around the town

where the recorded CCTV showed the Police stopping the drug-dealer (eleven samples) and rough ground with puddles and loose material at Dublin Airport Long Stay car-park (sixteen samples).

Initial laboratory analysis followed two routes: (1) rapid (for intelligence), comprising a non-destructive route of colour, grain-size, texture, pXRF (using a Bruker Instruments Tracer 5 device) and X-ray diffraction of all samples, followed by cone-and-quarter splitting: one half for microbiology using smear-slides (spores/pollen and testate amoebae), the other for subsequent microbiology and automated SEM-EDS mineralogy. Only the pXRF data and comments on the microbiology smear-slides are included here, as the aim of the first stage was to gain enough information to focus a search area of where the vehicle may have been. Geochemical (pXRF), mineralogical (XRD) and microbiology results were compared to regional maps of geochemistry (Tellus and TellusBorder databases); bedrock, superficial geology (geological surveys of Ireland and Northern Ireland); and land-use/plant types (European Union CORINE, environment agencies databases).

pXRF geochemistry from the soil obtained from the vehicle distinguished it from the other locations sampled, and indicated (from the regional databases, above) a Carboniferous limestone source, with few urban contaminants. This interpretation was supported by the XRD and microbiology data (Table 5). A significant amount of this bedrock occurs in a 50 km wide area between the missing person's home address and Dublin Airport. Pollen screening showed the presence of pine, maize, cannabis and various grasses. A combined map of the regional geochemical/geological and land-use in the swath, identified six locations of pine trees, on Carboniferous limestone (and derived glacial deposits/soils) with regular maize cultivation. Visits to these areas by police officers located a cannabis plantation within a maize field, with nearby vehicular access and down-wind (east of) the dominant regional air-flow through the region. At this location, personal items belonging to the missing person were located. A second phase of sampling at and around this location gathered sixteen samples. pXRF alone was sufficient to distinguish the samples from the vehicle from the other locations sampled but showed a comparison between the vehicle samples and those from the maize/pine/cannabis plantation on the basis of a combined consideration of Si, Al, K and Ti (Fig. 6).

Iron contents from the soils from the vehicle were considered as possibly derived from the vehicle itself. Cross-plots (Fig. 6) or canonical distributions of elemental content are a simple, visual means

Fig. 5. A Map of Ireland, showing locations considered in text (the geolocated possible origin of the vehicle samples is not shown, intentionally, but is between 'last seen' and 'vehicle abandoned'); B: vehicle underside, showing soil adherence and non-painted metal work; C and D: interpreted mud-spatter on the upper body work of vehicle.

Table 5
Averaged percentages of pXRF geochemical data (n = number) of soil samples taken from the missing person's home address and suspected route. See Table 1 for detection limits.

	SiO$_2$	Al$_2$O$_3$	MgO	S	K$_2$O	CaO	TiO$_2$	Fe$_2$O$_3$	Total
(a) *First Phase*									
Vehicle (n = 6)	35	26	0	1	8	3	2	5	80
Family home (n = 9)	11	14	0	8	0	2	0	1	37
Home address (n = 11)	46	19	6	1	0	6	1	5	85
Meeting Place (n = 11)	3	20	7	1	1	17	0	5	55
Dublin Carpark (n = 16)	36	18	4	2	1	18	0	7	87
(a) *Second Phase*									
Search Location (n = 15)	35	29	0	1	9	3	3	1	80

of data comparison, but do not consider the limits of pXRF measurement, such as peak overlaps (e.g. Pb and As; V and Cr or Fe and Co: [46]), as well as the environmental conditions from which the sample was obtained (e.g. Fe contents from vehicle parts or introduced contaminants in semi-urban locations such as car-parks).

Due to the dominance of one bedrock type (Carboniferous Limestone) through roughly two thirds of the area considered ('meeting place' to Dublin Airport), pXRF alone did not have the discriminatory power to allow accurate geolocation. A combination of pXRF with pollen analysis, as a rapid means of environmental
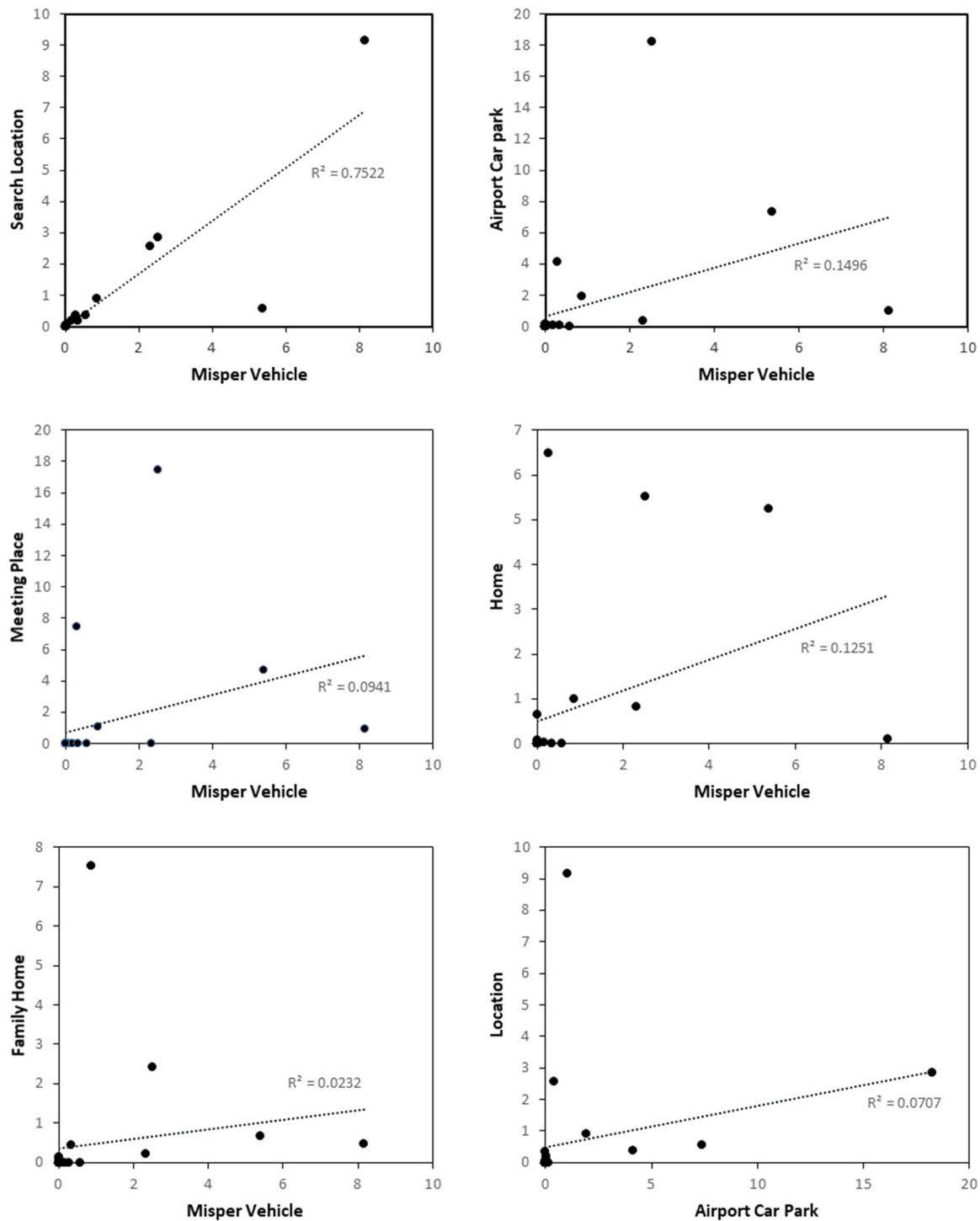
Fig. 6. Elementary cross-plots with root-square coefficents of derivation for simple Misper data comparison: such manipulation is effective, but without geochemical considerations (see text).

location, was however, sufficient in combination to reduce the possible search locations to a manageable number, allowing a further place to be added to police intelligence on the movements of the vehicle, and given the associated discovery of his personal items, where he may have been as well (they could have been discarded at the maize/pine/cannabis plantation). Given the limited time

between the CCTV record of the vehicle movement, and it's entry to the car-park, the mud-spatter on the vehicle likely came in these 9 h, or sometime prior to it, and not from a location near the Misper home locations. Precipitation and vehicle spray could have removed some of the soil spatter, and added further material, but no evidence to this effect was observed. To date, the Misper has not been located.

Fig. 7. Fragments of 'lignite bracelet' (bangles, herein) recovered from archaeological excavations in the north of Ireland. Left 'bangle' is ~8 cm top to base.

One of the key aspects of many forensic geoscience investigations is soil sampling and analysis, either to test whether or not there is an association between a known location and questioned soil samples, or as part of an intelligence driven analysis to determine an unknown geographical location from soil samples. Such intelligence-driven investigations can be time critical, such that rapid, non-destructive screening methods of analysis are of considerable value. In this case, careful sample extraction and analysis from the missing persons car, when combined with the specific case intelligence, identified potential search areas. In this way, search assets could then be deployed more effectively, in this case resulting in the recovery of items belonging to the missing person. In cases which are time critical, rapid screening methods are of significant value in an intelligence-driven operation.

2.5. Origin of Medieval lignite bangles case study

Various organic-rich, dark grey materials are known to have been used for ornamental purposes. Jet (a variety of lignite), coal and petrified wood (from peat bogs/lignite deposits) are fine-grained (producing a smooth, polishable finish), often homogenous (thus easy to work) and sometimes rare enough to be classified as semi-precious (like Whitby Jet). Dark grey, circular objects are common at archaeological sites from the Medieval in Ireland (Fig. 7, see [47]) and have been interpreted as bangles or bracelets. Over 700 bracelet fragments have been recovered from around 200 locations across Ireland. The majority of these artefacts have only been visually identified as lignite or jet but this in turn is used as an indicator of trade, exchange and communication networks, with inferences regarding local and foreign trade and exchange being drawn from their distribution patterns (e.g. [48]). These identifications are however,

problematic, given the difficulties in correctly identifying raw materials from visual inspection alone [49].

An excavation at St Patrick's Church, Armoy (County Antrim, N. Ireland) in 2004 and 2005, yielded abundant black, smooth bangles and parts thereof were located and preserved (Fig. 8). Armoy is located on Pleistocene glacial deposits, above Palaeogene basalts, but with peat bogs (possibly containing Irish Bog Oak), Neogene lignite (that contains petrified wood deposits) and Carboniferous coal deposits all nearby. In addition, these objects could have been imported. The aim of this study was to use pXRF to compare the excavated bangles to referenced Carboniferous coals and Neogene lignites from the Geological Survey of N. Ireland Core Store in order to include one or both of these as possible sources, or to exclude them and examine whether local bog oak or exotic coal/petrified wood or jet may be a possible source.

The main source of jet exploited in this period is likely to have been from Whitby in Yorkshire. Lignite is present in the geology of the Lough Neagh Group, however, the lignite seams subcrop the glacial and more recent deposits, which are up to tens of metres thick and lignite outcrops are not known in either of the main areas around Lough Neagh or at Ballymoney. A further potential source may have been the thin lignite beds that are sometimes found in the Inter-basaltic Formation, which occurs between the Upper and Lower Basalts in north Antrim. Coal and shale deposits exposed at the coast in Ballycastle, Co. Antrim may also have been a suitable source for the Armoy material.

In this case study, along with artefacts recovered during the excavations at Armoy, a range of artefacts were also selected from those held by the Historic Environment Division, Department for Communities in Belfast and in the teaching collection of the Archaeology Department at Queen's University Belfast. Elemental analysis was carried out on thirty-seven samples from eleven excavations using a portable X-ray Fluorescence (pXRF) Bruker S1 Turbo LE. The surface of each sample was cleaned and analysed three times on different areas of the piece and the results averaged. In order to provide comparative data, the same methodology was also applied to thirty-six geological samples from lignite, shale and coal cores held by the Geological Survey Northern Ireland.

The data indicate that the artefacts analysed were not in fact comparable with the lignite geological samples and were more comparable with the coal and shale samples (Fig. 9). Although a sample of jet was not available for inclusion in the study, the pXRF results indicate that none of the artefacts are jet, as typically jet has low levels of iron at less than 0.1% [49] and all of the artefacts tested had much higher levels of iron. Air should however, be noted that another possibility is that the significant sample burial time may have influenced the lignite composition and perhaps absorbed elements from the surrounding materials which may have caused the element discrepancies.

The results indicate that the material exploited at Armoy and other sites in the north of Ireland is more comparable with types of

Fig. 8. Waste from the presumed production of the bangles recovered during the excavation at Armoy, Co. Antrim. It is presumed the bangles were produced by creating discs and then removing the central core before polishing the resulting ring to a high shine. Diameter range (L-R) = ~6 cm to ~3 cm.
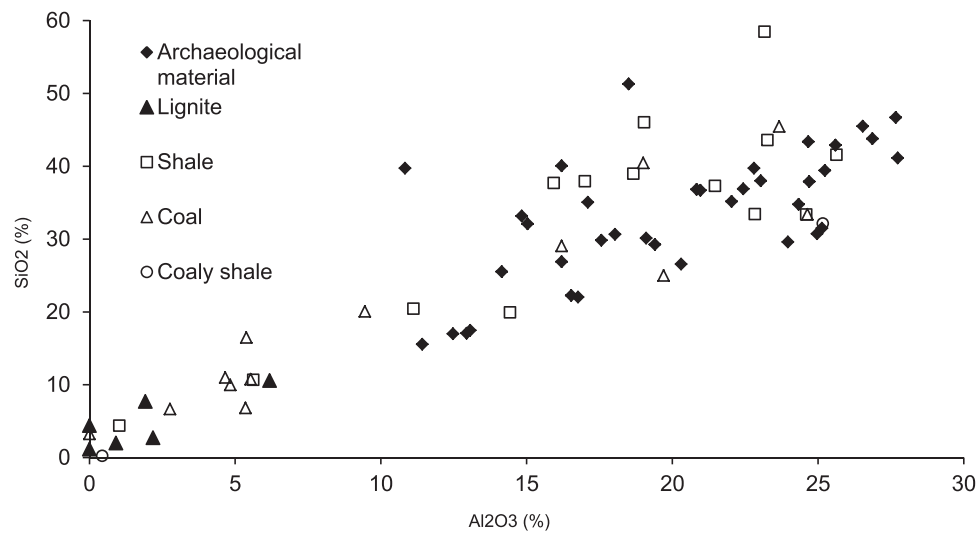
Fig. 9. Al$_2$O$_3$ vs SiO$_2$ content of lignite bangles and known geological samples of lignite, shale, coal and coaly shale from Northern Ireland.

coals and shale than lignite or jet. The Carboniferous shales which crop out on the north coast, near Ballycastle, for example, may have been a suitable source for the Armoy material.

2.6. Cremated remains case study: real or fake human cremated remains?

Cremating human remains is increasingly common globally; in Japan almost all burials are cremated, and cremation rates in at least twelve other countries, including South Korea, Canada, Switzerland, and the United Kingdom were > 70% in 2019 [50]. In the United States the cremation rate was 54.6% in 2019 and provisional data show 56.1% were cremated in 2020, continuing the two-decade 1.5% average yearly increase [51]. Reasons are varied, including scarcity of land, loosening of religious prohibitions, increasing popularity of green funeral practices and high cost of traditional burials [52,53]. The current global pandemic will impact statistics and change funerals moving forward, potentially accelerating the current trend.

As human cremation becomes common, the potential for mishandling, abuse and fraud also expands. In the United States the most famous recent instance of cremation fraud was the 2002 Tri-State Crematory case. Roughly two thousand bodies had been sent to the facility by local funeral homes but 334 bodies were disposed of inappropriately [54,55]. A significant number were appropriately cremated, while others were left in random locations on the property. This meant hundreds of families were uncertain as to the contents of their urns and regional crime laboratories were overwhelmed with questioned remains [24]. Analysis revealed some families had been given urns filled with a variety of filler materials, such as Portland cement or concrete powder, instead of cremated remains. However, differentiation of true human remains from other materials was hampered at the time by the lack of a clear basis for comparison [56,57]. The trace elemental composition of bone depends on multiple factors such as diet, the environment in which a person lives, and occupational exposures [58,59,60], and cremation can further alter the elemental composition [61]. There are increasing pressures to find reliable ways of distinguishing powdered bones from filler materials and developing ways of identifying

Fig. 10. Photographs of cremated human remains processed using (left) traditional ball/hammer mill and (right) rotary-blade processor. Note ball/hammer mill fragments are typically 4 mm in diameter.

cremated human remains. A rapid method of screening cremated human remains materials is thus of significant value.

In more recent years this challenge has been compounded by funeral industry changes. Common funeral practice has shifted from using ball/hammer mills to rotary-blade processing units to fit remains into funeral urns [62]. In the ball/hammer mill, remains are placed in a perforated steel drum and crushed into fragments small enough to fall through perforations, typically 4 mm in diameter, leaving 4 mm+ fragments still visibly identifiable as diagnostic tooth and bone fragments, including complete ear ossicles. However, according to Warren and Schultz [62], there was a recurring problem in which the volume of remains exceeded the capacity of funeral urns. To achieve more efficient packing, most North American crematoriums now use a rotary-blade style processer where remains are reduced to a non-diagnostic homogeneous powder, that is difficult, or even impossible, to determine if the remains are human-based [67] (Fig. 10). The colour of cremated human remain varies, depending on temperature, duration and proximity to heat source and the post-cremation environment [58,67]. Consequently, whilst cremated human remains are typically chalk-white to grey, other colours are possible. Thus, analytical methods are generally the most reliable way of identifying human cremated remains from other materials.

Table 6

pXRF selected element concentrations (270 s) for the questioned cremated human remains sample compared to the largest published elemental values for known human remains [4,7,34,66,72]. See Table 1 for detection limits.

	Cu (ppm)	Fe (ppm)	Mn (ppm)	Pb (ppm)	S (ppm)	Sr (ppm)	Zn (ppm)
Questioned Cremains	360	2,300	340	180	34,800	1,480	1,150
Largest value in literature	92.2	1,750	69.5	204.53	3,450	418	429
Approximat% difference	120	25	130	10	165	110	90

Some analytical techniques, such as ICP-OES [56], LA-ICP-SF-MS [68], and AA-MS [69], are destructive and only characterize selected elements, while others such as PIXE [70] can detect the required elements in one measurement at better accuracies than pXRF. XRF can detect potassium and calcium, is non-destructive, requires little sample preparation and distinguishes bioapatite (bone/teeth) from geologically occurring material (limestone/chalk/wood ash), by looking at the calcium/phosphate (Ca/P) ratios (ranging from 1.23 to 2.8) and concentrations of specific trace elements, e.g. heavy metals (Yoshinaga et al. [71,72,73]). Complications occur where remains may become contaminated by other materials, unusual occupations, or environmental exposure, leading to unusual trace elemental signatures [56] so XRD may be necessary for identification [71].

For pXRF analysis, subsamples taken using a stainless-steel scoop were placed into a sample cup lined with a 0.16 mil polypropylene film substrate, and filled to a depth of at least 20 mm. The sample cup was then gently tapped to loosely pack the sample, with extra added if the sample depth dropped below 15 mm. Samples were positioned inside a test stand and analyzed using a Niton XL3tGOLDD+ with a low power Ag anode X-ray tube and a Si PiN detector set in TestAllGeo mode, which allows for detection of phosphorus without using a vacuum. Each sample was analysed at least three times and repositioned between each run. Additional replicate measurements may be required depending on an evaluation of initial results. Typically, once analysis is complete the sample is returned to the original container, with the interior of the sample cup and film substrate carefully cleaned using a non-static brush.

Based on analysis of reference standards such as NIST 1400, NIST 1486, CCRMP Till-4 and USGS Ar-M2, an analysis time of 270 s was chosen. For phosphorous this typically achieves a recovery of 100% ± 30% recovery (or %D < 30%) and a %RSD of < 10% for samples with > 10%. The limit of quantification at this sampling time is approximately 3000 ppm. Under these conditions, the Ca/P of both

NIST 1400 bone ash and NIST 1486 bone meal is roughly 1.9. The Ca/P of known cremated human remains, processed using a ball/hammer mill was 1.7, and a rotary-blade ranged from 1.4 to 2.0, which differs significantly from common filler materials such as wood ash (26−65) or charcoal ash (> 200). Concrete, mortar, plaster of paris, sheetrock and grout samples analysed to date, all have phosphorous levels below limit of detection. If analysing through a plastic bag this can alter the Ca/P ratio (see more information on theory and attenuation effects in [74]).

In this case study, a sample purported to be cremated human remains returned a Ca/P ratio of 2.7, which, whilst high for cremated human remains, was not out of the realm of possibility. Thus, a review of selected trace elements was necessary for a determination [71,72,73]. As seen in Table 6 and Fig. 11, several trace element concentrations were significantly greater than the maximum previously published values for known human remains, several of which were due to unusual occupational exposures,therefore indicating that the sample was not cremated human remains but based on comparison to a library of reference materials, most probably a form of wood ash. The advantage of using pXRF was the rapid and non-destructive nature of the analysis.

2.7. Graveyard soil contamination and field vs laboratory case study: St. Johns Church, Staffs, UK

An environmental contamination study was undertaken at the long-established St. Johns Church of England graveyard in Keele, Staffordshire, UK to determine if the pXRF technique could be used to both rapidly detect and characterise heavy metal element contamination (e.g. resulting from lead-lined coffins and other metal bearing buried materials). Available burial records are from 1542 A.D. but records show the presence of an earlier Knights Templar Church on the same site. Recent research has suggested that
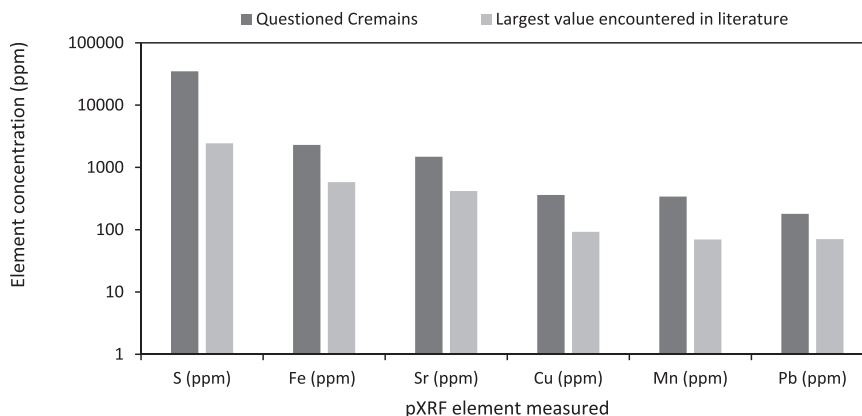

Fig. 11. Bar graph detailing selected element concentrations measured by the pXRF of questioned cremains and the largest values found in published literature. Note concentrations are on logarithmic scale.

Table 7
Descriptive statistics of in-situ surface soil (120 s) and laboratory soil pellets (300 s) selected heavy metal element concentration pXRF measurements, acquired from St, Johns Church graveyard, Keele, Staffordshire, UK. See Table 1 for detection limits.

Element	In-situ surface				Laboratory pellet				Control			
	Max. (ppm)	Min. (ppm)	Av. (ppm)	SD	Max. (ppm)	Min. (ppm)	Av. (ppm)	SD	Max. (ppm)	Min. (ppm)	Av. (ppm)	SD
Pb	305	30	120	77	1,540	130	395	340	90	25	50	25
Mn	1,910	210	615	452	1,625	105	1,625	685	1,350	550	1,105	120
Zn	180	40	65	33	385	40	130	80	85	30	70	20
Cr	55	15	35	11	115	40	65	20	125	70	100	25
As	80	10	31	10	20	5	10	5	15	5	10	5
Sr	55	15	35	11	125	50	65	16	95	50	75	20
Ba	855	55	225	154	2,735	310	695	470	680	350	530	150
Ca	58,190	340	6,560	155	164,330	1,240	19,160	39,775	580	3,440	1,725	415
P	1,460	180	600	290	930	2,650	1,520	395	975	645	820	60

burial grounds are effectively landfill [75] with there being little to no consistency with regards to environmental burial regulations within the U.K. and elsewhere, especially for heavy metal element concentrations although there is guidance for new burial grounds to take into account the location of local water sources, and post-mortem body fluid release, embalming fluids and pathogens/microbes [76]. Study results should provide information for follow-up, more detailed trace evidence investigations once anomalous heavy metal contaminated areas had been identified.

Field reconnaissance determined nine 10 m x 10 m potential sampling areas (i.e. avoiding dense vegetation/trees etc. which could not be sampled), which a random number generator then selected the specific sample positions to reduce potential sampling bias. At each sampling location, the overlying vegetation was removed to expose soil, checked for pebbles/vegetation and then analysed via pXRF for a 120 s measurement period. Surface soil samples were then taken for routine soil characterisation analysis including determination of average electrical conductivity following standard methodologies (47 µS/m). Soil moisture contents ranged from 16% to 24% and pH varied between 6 and 6.5. The surface soil samples were then prepared for laboratory XRF analysis following the methodology given in case study 1. Each pellet was then placed over the fixed aperture of the NITON XL3t 900 Analyzer in its laboratory holder and had a 300 s measurement time. Background control samples were also taken ~400 m away from the graveyard.

In-situ surface soil pXRF measurement results showed lead element concentration to vary from 30 ppm up to a maximum of 305 ppm with an average of 120 ppm (Table 7), with higher concentrations evidenced adjacent to the church itself (Fig. 12) and only 50 ppm in background control samples. Manganese had also high element concentration values up to 1910 ppm (Table 7) but distribution across the graveyard was more varied, when compared to lead element concentration distributions. Zinc had concentrations of 180 ppm down to 35 ppm about the same as background control samples. Arsenic had also high element concentrations values up to 80 ppm that were much higher than control values (Table 7). Calcium also had very high element concentrations up to 165,000 ppm compared to 1725 ppm in control samples.

The laboratory soil pellet pXRF measurement results from the same locations showed consistently higher heavy metal element concentrations, when compared to the in situ measurements (Table 7), most probably due to the removal of water in the laboratory samples, but the relative differences in element concentrations within the graveyard were found to be similar with both analysis methods.

This case study showed both in situ surface soil and subsequent laboratory analysis of soil pellet pXRF element concentrations datasets to have evidenced significant heavy metal element contamination. The laboratory measurement means all gave higher element concentrations, when compared to the surface measurements, most probably due to the removal of soil moisture in the laboratory samples. However, both datasets still gave relatively similar concentration variations across the study site. Moreover, the concentrations determined by both field and laboratory methods for Pb, the principal element of interest in the churchyard case study, are well above the typical ambient background concentrations observed in the soils of England and Wales (i.e. median 40 ppm, mean 74 ppm; [77]), thus indicating a level of contamination exists here. In addition, the mean concentrations determined by both the laboratory and field method are above the threshold level (75 ppm) identified for potential ecotoxicological effects in soils identified by deVries et al. [78] while in many of the sampling points examined the concentrations were also above the predicted no effect concentrations of 166 ppm and 212 ppm reported by Smolders et al. [79] and the European Chemicals Agency [80], respectively. This shows that the rapid analysis techniques can identify priority areas for
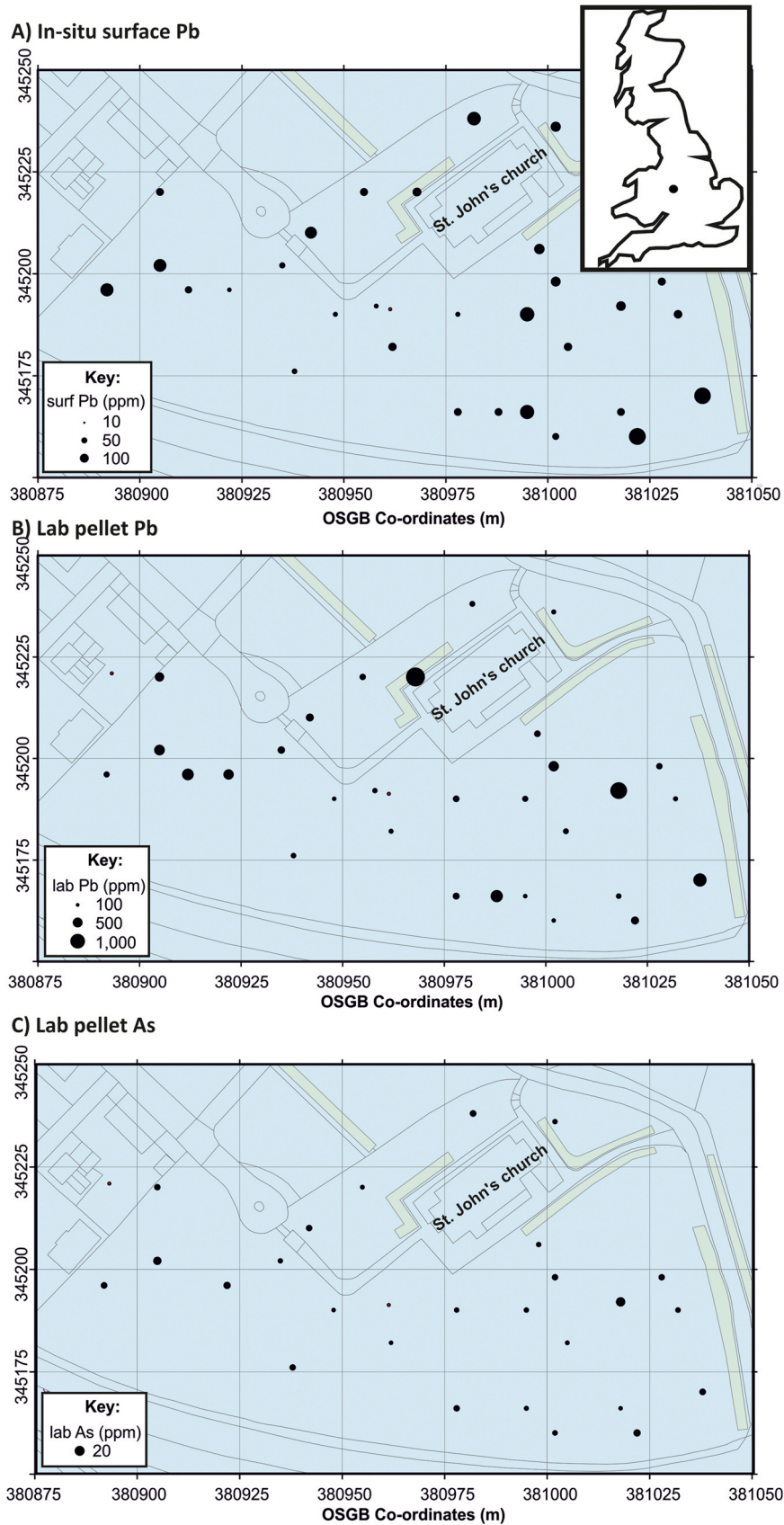
Fig. 12. St. John's Church graveyard, Keele, Staffs, UK with location map (inset). a) *In-situ* surface and b) laboratory soil pellet Lead element pXRF concentrations, and c) laboratory Arsenic element pXRF concentrations (see respective keys and text for more information).

urgent inspection. The rapidly acquired churchyard data obtained here also indicates that lead hot spots in the examined soil are not only associated with proximity to buildings and consequent leaching from for example, lead flashings and roof linings, but also with other point sources such as release from coffins. This in itself can guide future investigations and management decisions.

3. Conclusions and further work

In summary, pXRF surveys show great potential in forensic applications from the case studies shown in this paper. pXRF equipment is relatively cheap to acquire, when compared to other trace evidence methods, robust and portable in the field, with simple data collection and little processing required to pinpoint anomalous areas, as long as significant background measurements have been taken. It also shows great versatility to successfully be utilised for different forensic trace evidence purposes as shown by the case studies in this paper. pXRF limitations include (i) the observation that most site surveys will require measurements to be calibrated against standards, (ii) the need for longer sample measurements times to improve accuracy, (iii) the inability to measure elements lighter than aluminium and (iv) absolute concentration values require a lot more laboratory sample analysis using other techniques. Further research is suggested to validate these initial findings by comparing to more laboratory-based analytical methods where higher degrees of measurement accuracies can be obtained.

CRediT authorship contribution statement

Jamie Pringle: Conceptualisation, Writing – original draft, Writing – review & editing. **Adam Jeffery:** Methodology, Writing – review & editing. **Alastair Ruffell:** Case study, Writing - original draft. **Ian Stimpson:** Case study, Writing - review & editing. **Duncan Pirrie:** Writing - review & editing. **Elisa Bergslien**: Case study, Writing - original draft, Writing - review & editing. **Charlie Madden:** Conceptualisation, Case study, Writing - review & editing. **Ian Oliver:** Writing - review & editing. **Kris Wisniewski:** Case study, Writing - original draft, Writing - review and editing. **John Cassella:** Case study, Writing - review & editing. **Neil Lamont:** Case study, Writing - review & editing. **Sarah Gormley:** Case study, Writing - review & editing. **Julian Partridge:** Case study, Writing - review & editing.

Acknowledgements

Conflict of interest

None.

References

[1] D. Pirrie, A.J. Pidduck, D.E. Crean, T.M. Nicholls, Identification and analysis of man-made geological product particles to aid forensic investigation of provenance in the built environment, . Sci. Int. 305 (2019) 109974, https://doi.org/10.1016/j.forsciint.2019.109974

[2] D. Pirrie, A. Ruffell, L. Dawson, Geological evidence recovery from exhibits, in: L. Donnelly, D. Pirrie, M. Harrison, A. Ruffell, L. Dawson (Eds.), A Guide to Forensic Geology, Geological Society, London, 2021.

[3] D. Pirrie, A. Ruffell, L. Dawson, J. McKinley, Crime scenes: geoforensic assessment sampling and examination, in: L. Donnelly, D. Pirrie, M. Harrison, A. Ruffell, L. Dawson (Eds.), A Guide to Forensic Geology, Geological Society, London, 2021.

[4] A. Ruffell, L. Dawson, Forensic geology in environment crime: illegal waste movement and burial in Northern Ireland, Environ. For. 10 (2009) 1–6.

[5] D. Pirrie, Forensic geology in serious crime investigations, Geol. Today 25 (2009) 188–192.

[6] A.G. Brown, The use of forensic botany and geology in war crimes investigations in NE Bosnia, Forensic Sci. Int. 163 (2006) 204–210.

[7] S.C. Jantzi, J.R. Almirall, Characterization and forensic analysis of soil samples using laser-induced breakdown spectroscopy (LIBS), Anal. Bioanal. Chem. 400 (2011) 3341–3351.

[8] L. Reidy, K. Bu, M. Godfrey, J.V. Cizdziel, Elemental fingerprinting of soils using ICP-MS and multivariate statistics: A study for and by forensic chemistry majors, Forensic Sci. Int. 233 (2013) 37–44.

[9] C.N. Grant, J.M.R. Antoine, Instrumental neutron activation analysis in forensic science in Jamaica: The case of the Coral Springs beach theft, Forensic Chem. 7 (2018) 88–93.

[10] X. Xu, C. Du, F. Ma, Y. Shen, J. Zhou, Forensic soil analysis using laser-induced breakdown spectroscopy (LIBS) and Fourier transform infrared total attenuated reflectance spectroscopy (FTIR-ATR): principles and case studies, Forensic Sci. Int. 310 (2020).

[11] K. Langstraat, A. Knijnenberg, G. Edelman, L. van de Merwe, A. van Loon, J. Dik, A. van Asten, Large area imaging of forensic evidence with MA-XRF, Sci. Rep. 7 (2017) 15056.

[12] K.M. Pitts, R.M. Clarke, The forensic discrimination of quartz sands from the Swan Coastal Plain, Western Australia, Forensic Sci. Int. Rep. 2 (2020), https://doi.org/10.1016/j.fsir.2020.100130

[13] A. Ruffell, P. Wiltshire, Conjunctive use of quantitative and qualitative X-ray diffraction analysis of soils and rocks for forensic analysis, Forensic Sci. Int. 145 (1) (2004) 13–23.

[14] A. Ruffell, D. Pirrie, L. Dawson, Geological evidence analysis, in: L. Donnelly, D. Pirrie, M. Harrison, A. Ruffell, L. Dawson (Eds.), A Guide to Forensic Geology, Geological Society, London, 2021, p. 154.

[15] J. Morrison, G. Watts, G. Hobbs, N. Dawnay, Field-based detection of biological samples for forensic analysis: established techniques, novel tools, and future innovations, For.Sci. Int. 285 (2018) 147–160.

[16] A. Choodum, P. Kanatharana, W. Wongniramaikul, N. NicDaeid, Rapid quantitative colourimetric tests for trinitrotoluene (TNT) in soil, . Sci. Int. 222 (2012) 340–345.

[17] I. Ibarrondo, U. Balziskueta, I. Martínez-Arkarazo, C. García-Florentino, G. Arana, A. Azkarate, J.M. Madariaga, Portable Raman can be the new hammer for architects restoring 20th-century built heritage elements made of reinforced concrete, J. Raman Spectrosc. 52 (2021) 109–122.

[18] J.K. Pringle, A. Ruffell, J.R. Jervis, L. Donnelly, J. McKinley, J. Hansen, R. Morgan, D. Pirrie, M. Harrison, The use of geoscience methods for terrestrial forensic searches, Earth Sci. Rev. 114 (2012) 108–123.

[19] J.K. Pringle, K.D. Wisniewski, M. Giubertoni, N.J. Cassidy, J.D. Hansen, N.J. Linford, R.M. Daniels, The use of magnetic susceptibility as a forensic search tool, . Sci. Int. 246 (2015) 31–42.

[20] G.E.M. Hall, G.F. Bonham-Carter, A. Buchar, Evaluation of portable X-ray fluorescence (pXRF) in exploration and mining: phase 1, control reference materials, Geochem. Explor. Environ. Anal. 14 (2014) 99–123.

[21] A.E. Steiner, R.M. Conrey, J.A. Wolff, PXRF calibrations for volcanic rocks and the application of in-field analysis to the geosciences, Chem. Geol. 453 (2017) 35–54.

[22] R.N. Brent, H. Wines, J. Luther, N. Irving, J. Collins, B.L. Drake, Validation of handheld X-ray fluorescence for in situ measurement of mercury in soils, J. Env. Chem. Eng. 5 (2017) 768–776.

[23] D. Smith, Handheld X-ray fluorescence analysis of Renaissance bronzes: practical approaches to quantification and acquisition, in: A.N. Shugar, J.L. Mass (Eds.), Handheld XRF for Art and Archaeology, Leuven University Press, 2012, pp. 37–74.

[24] J.L. Smith, 10th anniversary of bodies discovered at Tri-State Crematory in Noble, Georgia. Times Free Press. February 12th, 2012b. http://www.timesfreepress.com/news/news/story/2012/feb/12/horror-in-noble/70497/ (Accessed 29 June 2021).

[25] C. McGlinchey, Handheld XRF for the examination of paintings: proper use and limitations, in: A.N. Shugar, J.L. Mass (Eds.), Handheld XRF for art and Archeology, University Press, Leuven, 2012, pp. 131–158.

[26] J.-H. Liang, P.-P. Liu, Z. Chen, G.-X. Sun, H. Li, Rapid evaluation of arsenic contamination in paddy soils using field portable x-ray fluorescence spectrometry, J. Environ. Sci. 64 (2018) 345–351.

[27] T. Radu, D. Diamond, Comparison of soil pollution concentrations determined using AAS and pXRF techniques, J. Hazard. Mat. 171 (2009) 1168–1171.

[28] M. Rouillon, M.P. Taylor, C. Dong, Reducing risk and increasing confidence of decision making at a lower cost: In-situ pXRF assessment of metal-contaminated sites, Environ. Pollut. 229 (2017) 780–789.

[29] M. Rincheval, D.R. Cohen, F.A. Hemmings, Biogeochemical mapping of metal contamination from mine tailings using field-portable XRF, Sci. Total Environ. 662 (2019) 404–413.

[30] Z. Kasztovsky, B. Maroti, I. Harsanyi, D. Parkanyi, V. Szilagyi, A comparative study of PGAA and pXRF used for non-destructive provenancing archaeological obsidian, Quat. Int. 468 (2018) 179–189.

[31] A. Michalowski, P. Niedzielski, M. Teska, K. Jakubowski, M. Zolkiewski, Archaeometrical studies of prehistoric pottery using portable ED-XRF, Measurement 159 (2020) 107758, https://doi.org/10.1016/j.measurement.2020.107758

[32] A. Turner, In situ elemental characterisation of marine microplastics by portable XRF, Mar. Poll. Bull. 124 (2017) 286–291.

[33] X. Zhang, A.J. Specht, E. Wells, M.G. Weisskopf, J. Weuve, L.H. Nie, Evaluation of a portable XRF device for in vivo quantification of lead in bone among a US populations, Sci. Total Environ. 753 (2021) 142351, https://doi.org/10.1016/j.scitotenv.2020.142351

[34] K. Nganvongpanit, K. Buddhachat, S. Klinhom, P. Kaewmong, C. Thitaram, P. Mahakkanukrauh, Determining comparative elemental profile using handheld XRF in humans, elephants, dogs and dolphins: preliminary study for species identification, . Sci. Int. 263 (2016) 101–106.

[35] A.M.W. Hunt, R.J. Speakman, Portable XRF analysis of archaeological sediments and ceramics, J. Archaeol. Sci. 53 (2015) 626–638.

[36] E. Frahm, R.C.P. Doonan, The technological versus methodological revolution of portable XRF in archaeology, J. Archaeol. Sci. 40 (2013) 1425–1434.

[37] J.R. Jervis, J.K. Pringle, A study of the affect of seasonal climatic factors on the electrical resistivity response of three experimental graves, J. Appl. Geophys. 108 (2014) 53–60.

[38] Y. Imanishi, A. Bando, S. Komatani, S.-I. Wada, K. Tsuji, Experimental parameters for XRF of soils, Adv. X ray Anal. 53 (2010) 248–255.

[39] C. Parsons, E.M. Grabulosa, E. Pili, G.H. Floor, G. Roman-Ross, L. Charlet, Quantification of trace arsenic in soils by field-portable X-ray fluorescence spectrometry: Considerations for sample preparation and measurement conditions, J. Hazard. Mater. 262 (2013) 1213–1222.

[40] J.T. Padilla, J. Hormes, H.M. Selim, Use of pXRF: effect of thickness and antecedent moisture of soils on measured concentration of trace elements, Geoderma 337 (2019) 143–149.

[41] D.J. Kalnicky, R. Singhvi, Field portable XRF analysis of environmental samples, J. Hazard. Mat. 83 (2001) 93–122.

[42] G. Certini, R. Scalenghe, W.I. Woods, The impact of warfare on the soil environment, Earth Sci. Rev. 127 (2013) 1–15, https://doi.org/10.1016/j.earscirev.2013.08.009

[43] P. Doyle, A. Bennett, Military Geography: terrain evaluation and the British Western Front 1914–1918, Geogr. J. 163 (1997) 1–24.

[44] A. Burger, I. Lichtscheidl, Strontium in the environment: review about reactions of plants towards stable and radioactive strontium isotopes, Sci. Total Environ. 653 (2019) 1458–1512.

[45] A.D. Booth, V. Vandeginste, D. Pike, R. Abbey, R.A. Clark, C.M. Green, N. Howland, Geochemical insight during archaeological geophysical exploration through in situ X-ray fluorescence spectrometry, Arch. Prosp. 24 (2017) 361–372.

[46] S. Piorek, Principles and applications of man-portable X-ray fluorescence spectrometry, Trends Anal. Chem. 13 (1994) 281–286.

[47] S. Gormley, 'Lignite bracelet' production in the north of Ireland: a reassessment, J. Ir. Archaeol. 26 (2017) 117–142.

[48] M. Comber, Trade and communication networks in early historic Ireland, J. Ir. Archaeol. 10 (2001) 73–92.

[49] F.J. Hunter, J.G. McDonnell, A.M. Pollard, C.R. Morris, C.C. Rowlands, The scientific identification of archaeological jet-like artefacts, Archaeometry 35 (1) (1993) 69–89.

[50] Cremation Society of Great Britain, 2019 International cremation statistics. ⟨https://www.cremation.org.uk/International-cremation-statistics-2019⟩ (Accessed 25 June 2021).

[51] Cremation Association of North America, 2021. CANA Annual statistics report 2021. ⟨https://cdn.ymaws.com/www.cremationassociation.org/resource/resmgr/members_statistics/StatisticsReport2021-short.pdf⟩ (accessed 29 June 2021).

[52] J. Barron, 2021. In a move away from tradition, cremations increase. New York Times. 10 August 2017. ⟨https://www.nytimes.com/2017/08/10/nyregion/cremations-increase-in-a-move-away-from-tradition.html⟩ (Accessed 29 June 2021).

[53] National Funeral Directors Association, 2021. Trends in funeral service. https://nfda.org/news/trends-in-funeral-service (Accessed 29 June 2021).

[54] Brett, 2021. Man in notorious crematory case free from prison: 334 decaying corpses were found at Tri-State Crematory in 2002. Atlanta Journal-Constitution 30 June 2016, p. B1 (Accessed 29 June 2021).

[55] D.A. Markiewicz, Few takers for fake cremains; GBI seeks 'closure' in crematory scandal; families conflicted, Atlanta J. Const. 10 (2005) 1B Metro New August.

[56] T.R. Brooks, T.E. Bodkin, G.E. Potts, S.A. Smullen, Elemental analysis of human cremains using ICP-OES to classify legitimate and contaminated cremains, J. Forensic Sci. 51 (2006) 967–973.

[57] P. Bush, E.T. Bergslien, M. Bush, Commentary on: elemental analysis of human cremains using ICP-OES to classify legitimate and contaminated cremains, J. Forensic Sci. 51 (5) (2006) 967–973.

[58] M. Harbeck, R. Schleuder, J. Schneider, I. Wiechmann, W.W. Schmahl, G. Grupe, Research potential and limitations of trace analyses of cremated remains, Forensic Sci. Int. 204 (1–3) (2011) 191–200, https://doi.org/10.1016/j.forsciint.2010.06.004

[59] J.S. Harkness, T.T. Darrah, From the crust to the cortical: the geochemistry of trace elements in human bone, Geochim. Cosmochim. Acta 249 (2019) 76–94, https://doi.org/10.1016/j.gca.2019.01.019

[60] B. Wopenka, J.D. Pasteris, A mineralogical perspective on the apatite in bone, Mater. Sci. Eng. C 25 (2005) 131–143.

[61] A.P. Mamede, D. Gonçalves, M.P.M. Marques, L.A.E. Batista de Carvalho, Burned bones tell their own stories: a review of methodological approaches to assess heat-induced diagenesis, Appl. Spect. Rev. 53 (8) (2018) 603–635, https://doi.org/10.1080/05704928.2017.1400442

[62] M.W. Warren, J.J. Schultz, Post-cremation taphonomy and artifact preservation, J. Forensic Sci. 47 (3) (2002) 656–659.

[63] I. Baranowska, K. Czernicki, R. Aleksandrowicz, R, The analysis of lead, cadmium, zinc, copper and nickel content in human bones from the Upper Silesian industrial district, 1995, Sci. Total Environ. 159 (1995) 155–162, https://doi.org/10.1016/0048-9697(95)04218-P

[64] G.V. Iyengar, L. Tandon, L. Minor, Trace Elements in Human Bones and Teeth. International Atomic Energy Agency, Section of Nutritional and Health-Related Environmental Studies, Vienna, Austria. NAHRES-39, 1999.

[65] J.R. Ščančar, M. Milačič, M. Benedik, P. Bukovec, Determination of trace elements and calcium in bone of the human iliac crest by atomic adsorption spectrometry, Clin. Chem. Acta 293 (2000) 187–197.

[66] Yoshiyuki Tohno, Setsuko Tohno, Masako Utsumi, Takeshi Minami, Masayo Ichii, Yuko Okazaki, Fumio Nishiwaki, et al., Age-independent constancy of mineral contents in human vertebra and auditory ossicle, Biol. Trace Elem. Res. 59 (1) (1997) 167–175.

[67] J.J. Schultz, M.W. Warren, J.S. Krigbaum, Analysis of human cremains, in: C.W. Schmidt, S.A. Symes (Eds.), The Analysis of Burned Human Remains, second ed., Academic Press, 2015, pp. 83–103.

[68] W. Castro, J. Hoogewerff, C. Latkoczy, J.R. Almirall, Application of laser ablation (LA-ICP-SF-MS) for the elemental analysis of bone and teeth samples for discrimination purposes, Forensic Sci. Int. 195 (1–3) (2010) 17–27, https://doi.org/10.1016/j.forsciint.2009.10.029

[69] B.L. Gulson, C.W. Jameson, B.R. Gillings, Stable lead isotopes in teeth as indicators of past domicile—a potential new tool in forensic science? J. Forensic Sci. 42 (5) (1997) 787–791.

[70] M.W. Warren, A.B. Falsetti, I.I. Kravchenko, F.E. Dunnam, H.A. Rinsvelt, W.R. Maples, Elemental analysis of bone: proton-induced X-ray emission testing in forensic cases, Forensic Sci. Int. 125 (2002) 37–41.

[71] E.T. Bergslien, M.A. Bush, P.J. Bush, Identification of cremains using x-ray diffraction spectroscopy and a comparison to trace element analysis, Forensic Sci. Int. 175 (2) (2008) 218–226, https://doi.org/10.1016/j.forsciint.2007.07.004

[72] A.M. Christensen, M.A. Smith, R.M. Thomas, Validation of X-ray fluorescence spectrometry for determining osseous or dental origin of unknown material, J. Forensic Sci. 57 (1) (2011) 47–51, https://doi.org/10.1111/j.1556-4029.2011.01941.x

[73] H.A. Zimmerman, J.J. Schultz, M.E. Sigman, Preliminary validation of handheld X-ray fluorescence spectrometry: distinguishing osseous and dental tissue from nonbone material of similar chemical composition, J. Forensic Sci. 60 (2) (2015) 382–390, https://doi.org/10.1111/1556-4029.12690

[74] E.T. Bergslien, Portable X-ray fluorescence (PXRF) spectrometry of earth materials: considerations for forensic analysis, in: R.W. Fitzpatrick, L.J. Donnelly (Eds.), Forensic Soil Science and Geology, Geological Society, 492 Special Publications, London, 2021, , https://doi.org/10.1144/SP492-2017-346

[75] S. Fiedler, J. Bruer, C.M. Pusch, S. Holley, J. Wahl, J. Ingwersen, M. Graw, Graveyards – special landfill, Sci. Total Environ. 419 (2012) 90–97.

[76] UK Department of the Environment, 2016. Cemeteries and burials: prevent groundwater pollution. ⟨https://www.gov.uk/guidance/cemeteries-and-burials-prevent-groundwater-pollution⟩. Last accessed: 07/05/2021.

[77] S.P. McGrath, F.J. Zhao, Ambient background metal concentrations for soils in England and Wales, The Environment Agency, Sci. Report: SC050054/SR (2006).

[78] W. de Vries, S. Lofts, E. Tipping, M. Meili, J.E. Groenenberg, G. Schütze, Impact of soil properties on critical concentrations of Cadmium, Lead, Copper, Zinc, and Mercury in soil and soil solution in view of ecotoxicological effects, Reviews of Environmental Contamination and Toxicology, 191 Springer, New York, 2007.

[79] E. Smolders, K. Oorts, P.V. Sprang, I. Schoeters, C.R. Janssen, S.P. McGrath, M.J. McLaughlin, Toxicity of trace metals in soil as affected by soil type and aging after contamination: using calibrated bioavailability models to set ecological soil standards, Environ. Toxicol. Chem. 28 (2009) 1633–1642.

[80] ECA. ⟨https://echa.europa.eu/registration-dossier/-/registered-dossier/16063/6/1⟩ (Accessed 19 July 2021).